Variable-Block-Length Joint Channel Estimation and Data Detection for Spatial Modulation Over Time-Varying Channels

Yuya Akiba, Takumi Ishihara, and Shinya Sugiura, *Senior Member, IEEE*

***Abstract*—We propose novel variable-block-length joint channel estimation and data detection for spatial modulation over time-varying channels, where the data frame is divided into multiple blocks, and channel state information (CSI) is estimated in a block-by-block manner. More specifically, in each block maximum-likelihood-based data detection and channel estimation are iteratively carried out, where the detected data block is used as a long pilot sequence to update CSI. Our simulation results demonstrate that the performance of the proposed scheme is capable of approaching that of a perfect-CSI scenario. Moreover, the proposed scheme outperforms the recent rectangular differential spatial modulation scheme, without any substantial cost in terms of the preamble overhead and detection complexity.**

***Index Terms*—Channel estimation, iterative detection, massive MIMO, spatial modulation, time-varying channel.**

I. Introduction

Massive multiple-input multiple-output (MIMO) is a promising technique for configuring high-speed wireless communications [1], [2]. With the aid of a high number of transmit antennas at a base station, spectral efficiency is significantly enhanced. However, the massive MIMO systems are typically imposed by several limitations, such as high energy consumption and channel estimation (CE) overhead.

Spatial modulation (SM) [3]–[6] is one of the MIMO techniques, which is capable of operating in a high-energy efficiency, even in a massive MIMO arrangement. These benefits are achieved with the aid of a single radio-frequency (RF) transmitter structure, where the static energy consumption is maintained to be significantly low regardless of the number of transmit antennas [7]. Furthermore, the SM transmitter does not require CSI feedback from the receiver, unlike the original massive MIMO downlink, relying on conjugate beamforming [1].

Precise CSI is typically necessary for reliable data detection (DD). In MIMO systems, the pilot overhead imposed by CE linearly increases upon increasing the number of antenna elements. The effects of CE errors in the time-invariant channel on the achievable performance of SM were investigated in [8], [9]. Furthermore, in [10], [11], the analytical bit error ratios (BERs) of SM under the assumption of time-varying channels were derived. More specifically, in [10], by assuming the presence of a channel correlation, the entire channel is estimated by sending a pilot sequence from a single transmit antenna element, while achieving a low computational complexity at the receiver. Also, Khattabi and Alkhawaldeh [11] investigated the BER performance of SM under the assumption of time-varying Rayleigh fading, where estimated channel at the beginning of each frame is used over the entire frame. In order to reduce the pilot overhead, while maintaining a high CE accuracy, semi-blind iterative joint CE and DD [12]–[15] were proposed. Another approach to reducing the pilot overhead of MIMO systems is to employ differential space-time coding (DSTC) and non-coherent detection [16]. In DSTC, two consecutive DSTC blocks allow the receiver to demodulate information without relying on any CE in a block-by-block manner. However, the DSTC scheme suffers from the noise-doubling effect over the perfect CSI (PCSI) counterpart. The single-RF square differential SM (DSM) scheme was developed for enabling block-by-block non-coherent detection [17]. Note that due to the use of square space-time codes, the achievable transmission rate of DSTC and DSM becomes low [5], [18], especially in the scenario of a high number of transmit antennas.

Most recently, the authors' group proposed rectangular DSM (RDSM) [18], which allows DSTC to operate with the aid of rectangular space-time codes, rather than square ones, hence enhancing the transmission rate of DSTC. However, in the RDSM scheme, the preamble added in the top of the frame is used for data detection over the whole frame. This principle intrinsically corresponds to semi-blind detection, rather than block-by-block non-coherent detection. Therefore, RDSM suffers from the detrimental effects of error propagation in each frame. These effects become explicit especially for rapidly time-varying channels.[1]

Against this backcloth, we propose variable-block-length semi-blind detection for single-RF SM over time-varying channels, where the estimated CSI in the previous block is updated with the aid of joint CE and DD. Furthermore, the proposed scheme subsumes the semi-blind iterative joint CE and DD [15] in its special case. The detection complexity of the proposed scheme is maintained to be sufficiently low while reducing the preamble overhead.

The remainder of this paper is organized as follows. In Section II, we provide the system model of the proposed scheme, and in Section III, we derive the mean-square error (MSE) bound of the CE. Section IV characterizes the computational complexity of the proposed scheme, while Section V provides our simulation results. Finally, Section VI concludes this paper.

II. System Model

In this section, we first review the conventional semi-blind joint CE and DD scheme [15]. Then, the system model of the proposed scheme is presented.

A. Semi-Blind Joint CE and DD [15]

The semi-blind joint CE and DD was developed for the receiver of the SM scheme. At the SM transmitter, information bits are modulated

Manuscript received February 21, 2020; revised June 27, 2020 and August 31, 2020; accepted September 9, 2020. Date of publication September 14, 2020; date of current version November 12, 2020. This work was supported in part by the Japan Society for the Promotion of Science (JSPS) KAKENHI under Grants 16KK0120, 17H03259, and 17K18871, in part by the Japan Science and Technology Agency (JST) PRESTO under Grant JPMJPR1933. The review of this article was coordinated by Prof. Ha H. Nguyen. *(Corresponding author: Shinya Sugiura.)*

Yuya Akiba is with the Department of Computer and Information Sciences, Tokyo University of Agriculture and Technology, Koganei 184-8588, Japan (e-mail: s192810z@st.go.tuat.ac.jp).

Takumi Ishihara and Shinya Sugiura are with the Institute of Industrial Science, University of Tokyo, Tokyo 153-8505, Japan (e-mail: t.ishihara@ieee.org; sugiura@ieee.org).

Digital Object Identifier 10.1109/TVT.2020.3023718

[1]More specifically, the pilot overhead of semi-blind joint CE and DD [15] and RDSM [18] is identical. As for detection performance, the semi-blind CE and DD outperforms RDSM in the quasi-static channels, while RDSM exhibits a performance gain over the semi-blind CE and DD in the time-varying channel. However, both the schemes do not work in rapidly time-varying channels due to the presence of error propagation.

based on two principles, i.e., antenna activation and symbol constellation. An SM symbol is represented by

$$\mathbf{s}(t) = [0 \cdots 0 \underbrace{s(t)}_{m\text{th}} 0 \cdots 0]^T \in \mathbb{C}^M, \tag{1}$$

where M is the number of transmit antenna. Furthermore, $s(t) \in \mathbb{C}$ is a complex-valued symbol, modulated from L-point phase-shift keying (PSK) and quadrature amplitude modulation (QAM) constellations, and $m\,(1 \le m \le M)$ is the index of an activated antenna. Also, t is the symbol index in a T-length frame. Hence, the transmission rate is represented by $R = \log_2 L + \log_2 M$ [bps/Hz]. Under the assumption of time-varying frequency-flat fading channels, the received signals are given by

$$\mathbf{y}(t) = \mathbf{H}(t)\mathbf{s}(t) + \mathbf{v}(t), \tag{2}$$

where $\mathbf{H}(t) \in \mathbb{C}^{N\times M}$ are the channel gain matrix, whose nth-row and mth-column element corresponds to the channel between the mth transmit antenna and the nth receive antenna. Furthermore, the Jakes model can be used for generating the time-varying Rayleigh fading channels, similar to [18]. More specifically, the nth-row and mth-column element of $\mathbf{H}(t)$ was calculated by

$$\frac{1}{\sqrt{N_\mathrm{s}}}\left(\sum_{n=1}^{N_\mathrm{s}} \cos\left[2\pi\cos(\xi_{m,n})F_d T_s t + \zeta_{m,n}\right] + j\sum_{n=1}^{N_\mathrm{s}} \sin\left[2\pi\cos(\xi_{m,n})F_d T_s t + \bar{\zeta}_{m,n}\right]\right), \tag{3}$$

where N_s is the number of scatters, while $\xi_{m,n}$, $\zeta_{m,n}$, and $\bar{\zeta}_{m,n}$ are random variables, which are uniformly distributed over $[0, 2\pi]$. Moreover, N is the number of receive antennas, and $\mathbf{v}(t) \in \mathbb{C}^N$ is the associated additive white Gaussian noise (AWGN) component, which is generated as a random variable, obeying the complex-valued Gaussian distribution with a mean zero and a variance of σ^2.

In the conventional semi-blind joint CE and DD [15], the channel coefficients are assumed to be static over a frame, i.e. $\mathbf{H}(t) = \mathbf{H}$. The receiver estimates the initial CSI based on the pilot sequence $\mathbf{S}_p \in \mathbb{C}^{M\times M}$, added in the top of SM symbols, as follows:

$$\begin{aligned}\hat{\mathbf{H}}_0 &= \mathbf{Y}_p\mathbf{S}_p^+ \\ &= \mathbf{Y}_p\mathbf{S}_p^H\left(\mathbf{S}_p\mathbf{S}_p^H\right)^{-1},\end{aligned} \tag{4}$$

where $\mathbf{Y}_p$ is the received signals corresponding to the pilot symbols $\mathbf{S}_p$, $(\cdot)^+$ represents Moore-Penrose pseudo-inverse operation [19], and $(\cdot)^H$ represents Hermitian transpose. For simplicity, we employed the $(M \times M)$-sized identity matrix $\mathbf{I}_M$ for the pilot symbols $\mathbf{S}_p$. Then, based on maximum likelihood (ML) detection, the data symbols demodulated in the ith iteration are given by

$$\hat{\mathbf{s}}_i(t) = \arg\min_{\mathbf{s}} \left\|\mathbf{y}(t) - \hat{\mathbf{H}}_{i-1}\mathbf{s}\right\|^2 \ (i \ge 1), \tag{5}$$

where the estimated CSI in the ith iteration is denoted by $\hat{\mathbf{H}}_i$, and the initial condition of $\hat{\mathbf{H}}_i$ is set to $\hat{\mathbf{H}}_0$. Next, in the ith iteration, the CSI is updated by regarding $\hat{\mathbf{S}}_i = [\hat{\mathbf{s}}_i(1), \ldots, \hat{\mathbf{s}}_i(T)] \in \mathbb{C}^{M\times T}$ as a long pilot sequence as follows:

$$\hat{\mathbf{H}}_i = \mathbf{Y}\hat{\mathbf{S}}_i^H\left(\hat{\mathbf{S}}_i\hat{\mathbf{S}}_i^H\right)^{-1}, \tag{6}$$

where we have $\mathbf{Y} = [\mathbf{y}(1), \ldots, \mathbf{y}(T)] \in \mathbb{C}^{N\times T}$, and the maximum number of iterations is given by I_itr. The refined CSI allows us to further improve the demodulation performance.

Note that the computational complexity of the conventional semi-blind joint CE and DD [15], which is evaluated in terms of real-valued multiplications, is given by $(I_\mathrm{itr}+1)6N2^R + I_\mathrm{itr}(2+4N)$, where the first term corresponds to the complexity of ML detection (5), while the second term represents that of CE (6).

B. Proposed Variable-Block-Length Joint CE and DD

At the receiver, the T SM symbols per frame are divided into Q blocks, each having K symbols. Hence, we have the relationship of $T = QK$. In each block, the joint CE and DD is carried out, where the CSI estimated in the previous block is used as the initial CSI. This ensures that the proposed CE scheme is capable of tracking the rapid change of the channel coefficients. Let us denote the estimated CSI in the qth block and in the ith iteration as $\hat{\mathbf{H}}_{q,i}$ $(1 \le q \le Q, 1 \le i \le I_\mathrm{itr})$, while CSI estimated by the pilot block according to (4) is given by $\hat{\mathbf{H}}_{0,I_\mathrm{itr}}$.

In the qth block, the initial CSI $\hat{\mathbf{H}}_{q,0}$ is set to that estimated in the previous block $\hat{\mathbf{H}}_{q-1,I_\mathrm{itr}}$. Then, in the ith iteration, the data symbols are detected with the aid of ML detection as follows:

$$\hat{\mathbf{s}}_{q,i}(k) = \arg\min_{\mathbf{s}} \|\mathbf{y}((q-1)K+k) - \hat{\mathbf{H}}_{q,i-1}\mathbf{s}\|^2. \tag{7}$$

Then, based on the detected data symbols of (7), the CSI $\hat{\mathbf{H}}_{q,i}$ in the ith iteration and qth block is estimated as follows:

$$\hat{\mathbf{H}}_{q,i} = \mathbf{Y}_q\hat{\mathbf{S}}_{q,i}^+ + \hat{\mathbf{H}}_{q,i-1}\left(\mathbf{I}_M - \hat{\mathbf{S}}_{q,i}\hat{\mathbf{S}}_{q,i}^+\right), \tag{8}$$

where we have $\mathbf{Y}_q = [\mathbf{y}((q-1)K+1), \ldots, \mathbf{y}(qK)] \in \mathbb{C}^{N\times K}$ and $\hat{\mathbf{S}}_{q,i} = [\hat{s}_{q,i}((q-1)K+1), \ldots, \hat{s}_{q,i}(qK)] \in \mathbb{C}^{M\times K}$. In (8), the first term corresponds to the updated CSI coefficients, while the second term represents the non-updated ones.

The iteration between (7) and (8) is repeated up to I_itr times. Furthermore, $\hat{\mathbf{S}}_{q,i}^+$ is the pseudo-inverse operation of $\hat{\mathbf{S}}_{q,i}^+ = \hat{\mathbf{S}}_{q,i}^H(\hat{\mathbf{S}}_{q,i}\hat{\mathbf{S}}_{q,i}^H)^{-1}$ [19], which typically requires the highly-complex singular value decomposition. However, in the SM scheme, $\hat{\mathbf{S}}_{q,i}\hat{\mathbf{S}}_{q,i}^H \in \mathbb{C}^{M\times M}$ becomes a diagonal matrix since each column of $\hat{\mathbf{S}}_{q,i}$ has a single non-zero element. Hence, $(\hat{\mathbf{S}}_{q,i}\hat{\mathbf{S}}_{q,i}^H)^{-1}$ is calculated simply by inverting each diagonal element of $\hat{\mathbf{S}}_{q,i}\hat{\mathbf{S}}_{q,i}^H$. Hence, the mth-column elements of (8) are expressed as follows:

$$\left[\hat{\mathbf{H}}_{q,i}\right]_m = \begin{cases} \left[\hat{\mathbf{H}}_{q,i-1}\right]_m & \text{if } s_{q,i}(m) = 0 \\ \frac{\left[\mathbf{Y}_q\hat{\mathbf{S}}_{q,i}^H\right]_m}{|s_{q,i}(m)|^2} & \text{otherwise} \end{cases}, \tag{9}$$

where $[\cdot]_m$ denotes the mth column of a matrix.

III. MSE Bounds for CE

The MSE of CE errors is defined by

$$J = \frac{1}{MNQK}\sum_{q=1}^{Q}\sum_{t=(q-1)K+1}^{qK}\mathbb{E}\left[\left\|\mathbf{H}(t) - \hat{\mathbf{H}}_{q,I_\mathrm{itr}}\right\|^2\right]. \tag{10}$$

First, we derive the bounds of the MSE of CE, according to [13]. For simplicity, we assume that DD is error-free, and that each data block $\mathbf{S}_q$ is row full rank. From (2), we have

$$\mathbf{Y}_q = \tilde{\mathbf{H}}_q\tilde{\mathbf{S}}_q + \mathbf{V}_q, \tag{11}$$

where

$$\tilde{\mathbf{H}}_q = [\mathbf{H}((q-1)K+1), \ldots, \mathbf{H}(qK)] \in \mathbb{C}^{N\times MK} \tag{12}$$

$$\tilde{\mathbf{S}}_q = \begin{bmatrix} \mathbf{s}((q-1)K+1) & & \mathbf{0} \\ & \ddots & \\ \mathbf{0} & & \mathbf{s}(qK) \end{bmatrix} \in \mathbb{C}^{MK \times K} \quad (13)$$

$$\mathbf{V}_q = [\mathbf{v}((q-1)K+1), \ldots, \mathbf{v}(qK)] \in \mathbb{C}^{N \times K}. \quad (14)$$

Under the assumption of perfect DD, $\hat{\mathbf{S}}_q$ are regarded as

$$\begin{aligned} \hat{\mathbf{S}}_q &= \mathbf{S}_q \\ &= [\mathbf{s}((q-1)K+1), \ldots, \mathbf{s}(qK)] \in \mathbb{C}^{M \times K} \end{aligned} \quad (15)$$

By substituting (11) into (8), we have

$$\hat{\mathbf{H}}_{q,I_{\text{itr}}} = \tilde{\mathbf{H}}_q \tilde{\mathbf{S}}_q \mathbf{S}_q^H \left(\mathbf{S}_q \mathbf{S}_q^H\right)^{-1} + \mathbf{V}_q \mathbf{S}_q^H \left(\mathbf{S}_q \mathbf{S}_q^H\right)^{-1}. \quad (16)$$

Based on (12), (13), and (15), the first term of (16) is rewritten by

$$\begin{aligned} \bar{\mathbf{H}}_q &= \tilde{\mathbf{H}}_q \tilde{\mathbf{S}}_q \mathbf{S}_q^H \left(\mathbf{S}_q \mathbf{S}_q^H\right)^{-1} \\ &= \sum_{t=(q-1)K+1}^{qK} \mathbf{H}(t)\mathbf{s}(t)\mathbf{s}^H(t) \left(\sum_{t=(q-1)K+1}^{qK} \mathbf{s}(t)\mathbf{s}^H(t) \right)^{-1}. \end{aligned}$$

Then, we arrive at

$$\begin{aligned} \mathbb{E}\left[\left\| \mathbf{H}(t) - \hat{\mathbf{H}}_{q,I_{\text{itr}}} \right\|^2 \right] &\approx \mathbb{E}\left[\left\| \mathbf{H}(t) - \bar{\mathbf{H}}_q \right\|^2 \right] \\ &- \mathbb{E}\left[\text{tr}\left(\left(\mathbf{H}(t) - \bar{\mathbf{H}}_q\right) \left(\mathbf{S}_q \mathbf{S}_q^H\right)^{-1} \mathbf{S}_q \mathbf{V}_q^H \right) \right] \\ &- \mathbb{E}\left[\text{tr}\left(\mathbf{V}_q \mathbf{S}_q^H \left(\mathbf{S}_q \mathbf{S}_q^H\right)^{-1} \left(\mathbf{H}(t) - \bar{\mathbf{H}}_q\right)^H \right) \right] \\ &+ \mathbb{E}\left[\left\| \mathbf{V}_q \mathbf{S}_q^H \left(\mathbf{S}_q \mathbf{S}_q^H\right)^{-1} \right\|^2 \right]. \end{aligned} \quad (17)$$

The second and the third terms of (17) vanish because of the expectations of uncorrelated noise components. Additionally, according to [13], we consider the approximation of $\mathbf{S}_q \mathbf{S}_q^H \approx (K/M)\mathbf{I}_M$, which is almost satisfied for a sufficiently high M/K. Then, the fourth term of (17) is simplified to $M^2 N \sigma^2 / K$. Then, we have the bound of

$$J_1 = \frac{1}{MNQK} \sum_{q=1}^{Q} \sum_{t=(q-1)K+1}^{qK} \mathbb{E}\left[\left\| \mathbf{H}(t) - \bar{\mathbf{H}}_q \right\|^2 \right] + \frac{M\sigma^2}{K}. \quad (18)$$

The first term of (18) represents the CE errors induced by the time-varying channel, while the second term denotes that induced by the AWGN. Hence, by ignoring the effects of the channel's time variations, we obtain the loose closed-form bound of

$$J_2 = \frac{M\sigma^2}{K}. \quad (19)$$

Figs. 1(a) and 1(b) show the effects of the block length K on the MSE of CE in the proposed QPSK-modulated SM scheme, employing $(M, N) = (4, 4)$ and $(M, N) = (256, 4)$ antenna elements, respectively. In addition to the simulated curves of J, we also plotted the bounds of J_1 and J_2.

In Fig. 1(a), the frame length was given by $T = 300$, and the corresponding transmission rate was $R = 4$ [bps/Hz]. Furthermore, the block length was varied from $K = 20$ to 300, while the SNR was given by 10 dB, 15 dB, and 20 dB. The normalized Doppler frequency was set to $F_d T_s = 10^{-4}$. Observe in Fig. 1(a) that in each SNR scenario, there was a specific $K(< T)$ value, which minimizes the MSE. This implies

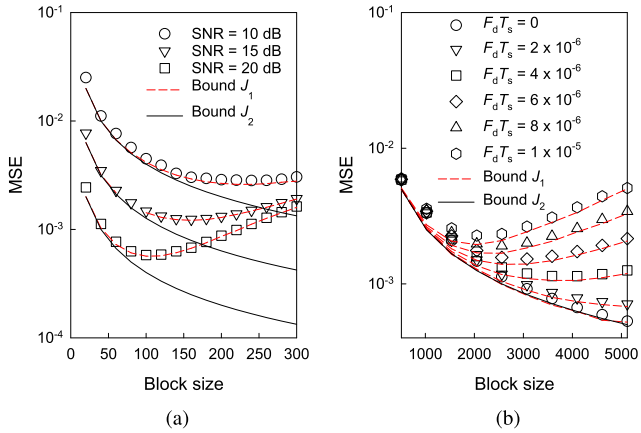

Fig. 1. The effects of the block length K on the MSE of CE; (a) $(M, N) = (4, 4)$, $T = 300$, and $F_d T_s = 10^{-4}$, (b) $(M, N) = (256, 4)$, $T = 5120$, and SNR $= 20$ dB.

that the CE performance of the proposed scheme is higher than the conventional joint CE and DD [15], which corresponds to the proposed scheme with $K = T = 300$. The bound of J_1 matched well with the simulated curves. This implies that our assumption of error-free DD is valid for deriving the tight MSE bound J_1. Furthermore, the CE performance of the proposed scheme was close to the bound J_2 in the low K regime, since CSI is updated more frequently than the effective channel's coherence time.

In Fig. 1(b), the block length K was varied from 512 to 5120, while the normalized Doppler frequency $F_d T_s$ was ranged from 0 to 1×10^{-5}. The SNR was fixed to 20 dB, and the frame length was given by $T = 5120$. As seen in Fig. 1(b), the optimal K value is equal to the frame size T, when $F_d T_s \leq 2 \times 10^{-6}$, which corresponds to the conventional joint CE and DD [15]. However, upon increasing the normalized Doppler frequency, the proposed scheme with the optimal K value exhibited lower MSE than the conventional semi-blind CE and DD scheme ($K = 5120$).

IV. Computational Complexity

In this section, we analyze the computational complexity imposed on the proposed receiver, which is evaluated in terms of the number of real-valued multiplications per time slot.

In the proposed scheme, $\hat{\mathbf{S}}_{q,i} \hat{\mathbf{S}}_{q,i}^H$ requires two real-valued multiplications per time slot, noting that each column of $\hat{\mathbf{S}}_{q,i}$ has a only single non-zero element. Also, $\mathbf{Y}_q \hat{\mathbf{S}}_{q,i}^H$ imposes $4N$ real-valued multiplications. Moreover, $[\mathbf{Y}_q \hat{\mathbf{S}}_{q,i}^H]_m / |s_{q,i}^{(m)}|^2$ $(1 \leq m \leq M)$ in (9) requires $2MN/K$ real-valued divisions per time slot. Additionally, ML detection requires $6N2^R$ real-valued multiplications [18]. Finally, by considering I_{itr} iterations, we obtain the total complexity of $(I_{\text{itr}} + 1)6N2^R + I_{\text{itr}}(2 + 4N + 2MN/K)$. The complexity associated with ML detection is dominant, and hence the proposed receiver's complexity is close to that of the conventional semi-blind joint CE and DD [15] for $K \gg MN$. In contrast, the computational complexity imposed by the coherent SM scheme, the RDSM scheme, the square DSTC scheme, and the square DSM scheme are given by $6N2^R$, $6N2^R + 4N(M+1)$, $2N(2M+1)2^{MR}$, and $6N2^{MR}$, respectively.

Fig. 2 compares the computational complexities of the proposed scheme and the related schemes. The number of transmit antennas was varied from $M = 2$ to 1024, where the transmission rate was given by

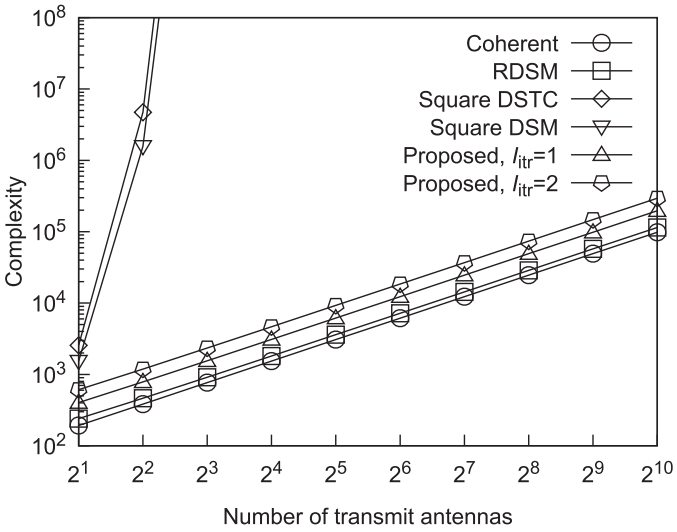

Fig. 2. Computational complexity comparison of the proposed scheme and the benchmarks. The number of receive antennas was $N = 4$, the transmission rate was given by $R = 2 + \log_2 M$ and the block length was $K = 256$.

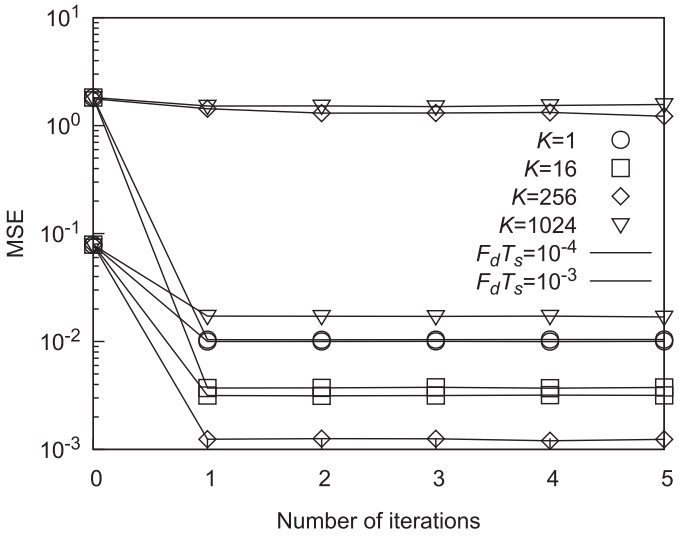

Fig. 3. The convergence behavior of the proposed scheme with $(M, N) = (4, 4)$. The transmission rate was $R = 4$ [bps/Hz], the frame length was given by $T = 1024$, and the SNR was 20 dB.

$R = 2 + \log_2 M$ [bps/Hz], while the number of receive antennas was fixed to $N = 4$. The block length was $K = 256$, and the number of iterations was $I_{\text{itr}} = 1$ and 2 for the proposed scheme. As seen in Fig. 2, the complexity of the proposed scheme was comparable to and slightly higher than those of the RDSM and the coherent SM schemes. This small gap is owing to the fact that the proposed scheme employs the iterative process between CE and DD, while the RDSM and the coherent SM schemes do not. By contrast, the complexities of the square DSTC and the square DSM schemes become prohibitively high for a high rate, as mentioned in [18].[2]

Note that the incorporation of the sphere decoding algorithm [20] into the proposed scheme is useful for further reducing the computational complexity.

V. Simulation Results

In this section, we provide our simulation results. The number of receive antennas was fixed to $N = 4$, and the QPSK modulation was employed for the proposed scheme. We maintained the relationship of $Q = \lceil T/K \rceil$. The Jakes model of (3) was employed for generating the time-varying Rayleigh fading channels.

A. Scenario of Low Number of Transmit Antennas ($M = 4$)

We considered the scenario of the low number of transmit antennas, where we have $M = 4$ and $R = 4$ [bps/Hz]. The frame length was given by $T = 1024$, and the pilot insertion rate was as low as $M/(M + KQ) \leq 0.39\%$.

In Fig. 3, we investigated the convergence behavior of the proposed scheme. The block length was set to $K = 1, 16, 256$, and 1024 for the normalized Doppler frequencies of $F_dT_s = 10^{-4}$ and 10^{-3}, and the SNR was given by 20 dB. Observe in Fig. 3 that only an $I_{\text{itr}} = 1$ iteration is sufficient for the convergence of MSE, similar to the conventional semi-blind CE and DD scheme [15].

Next, Figs. 4(a) and 4(b) show the BERs of the proposed scheme and the benchmark schemes, where the normalized Doppler frequency was given by $F_dT_s = 10^{-4}$ and 10^{-3}, respectively. The block length was set to $K = 256, 512$, and 1024 in Fig. 4(a), while we have $K = 16, 32$, and 64 in Fig. 4(b). The benchmarks were the coherent SM scheme with PCSI, the RDSM scheme, and the square DSM scheme. The system parameters of the square DSM scheme were given by $(L, Q) = (8, 16)$. As shown in Fig. 4(a), the BER curve of the proposed scheme with the block length of $K = 256$ nearly achieved that of the PCSI bound, while the conventional semi-blind joint CE and DD scheme [15], which corresponded to the proposed scheme with $K = 1024$, exhibited an error floor. To be more specific, this is because in the proposed scheme, upon increasing the block size K, the capability of tracking the time-varying channel with a high Doppler frequency became low, hence exhibiting an error floor. Moreover, the proposed scheme with $K = 256$ outperformed the RDSM scheme, where the performance gap was 1.3 dB at the BER of 10^{-4}. Note that the proposed and the RDSM schemes had the same amount of preamble overhead.

It is shown in Fig. 4(b) that the best K value of the proposed scheme depended on the SNR, as predicted from Fig. 1(a). More specifically, the best K value was $K = 32$ for the SNR < 15 dB and $K = 16$ for the SNR ≥ 15 dB. Also, the performance advantage of the proposed scheme over the RDSM scheme increased to approximately 2.0 dB at the BER of 10^{-4} in comparison to the lower normalized Doppler frequency scenario of Fig. 4(a).

To elaborate further, the proposed scheme subsumes the scheme of [15] as its special case of $K = T$. Hence, as a result of K optimization, the proposed scheme may coincide with the scheme of [15]. This tends to be true, especially in the scenarios of a low Doppler frequency and a high SNR. By contrast, our main target is to achieve an SM scheme's high performance in a rapidly time-varying scenario, where the scheme of [15] and RDSM exhibit an error floor, as shown in Figs. 4(a) and 4(b).

[2]To provide further insight, in Fig. 2 the effects of the number of transmit antennas M on the computational complexity were investigated, by assuming $R = \log_2 L + \log_2 M$. Naturally, the same trend holds true for the relationship between the constellation size L and the computational complexity.

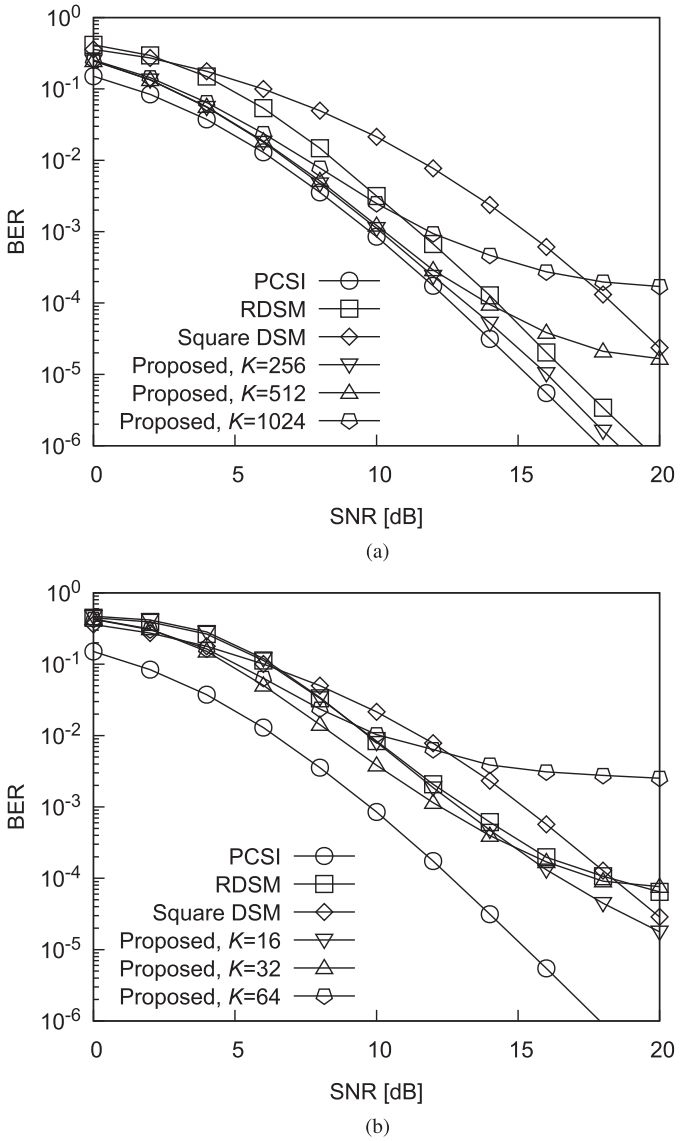

Fig. 4. The BER performance of the proposed scheme with $(M, N) = (4, 4)$. The frame length was given by $T = 1024$, and the transmission rate was $R = 4$ [bps/Hz]. (a) $F_d T_s = 10^{-4}$. (b) $F_d T_s = 10^{-3}$.

B. Massive MIMO Scenario ($M = 256$)

Next, we considered the massive MIMO scenarios with $M = 256$ transmit antennas, which corresponds to the transmission rate was $R = 10$ [bps/Hz].

In Fig. 5, we compared the BERs of the proposed scheme, the RDSM scheme, and the coherent SM scheme with PCSI. Here, the block length K of the proposed scheme was optimized at each SNR, such that the BER was minimized. The normalized Doppler frequency was set to $F_d T_s = 10^{-5}$, while the frame length was given by $T = 5120$, where the corresponding pilot insertion rate was lower than or equal to 4.8%. As seen in Fig. 5, the proposed scheme exhibited 2.0 dB better performance than the RDSM scheme at BER of 10^{-4}.

While in this paper we considered the performance improvement of the SM scheme in the scenario of rapidly time-varying channels, the proposed joint CE and DD scheme may be readily applicable to the frequency-domain index modulation [21] and its generalized counterpart [22].

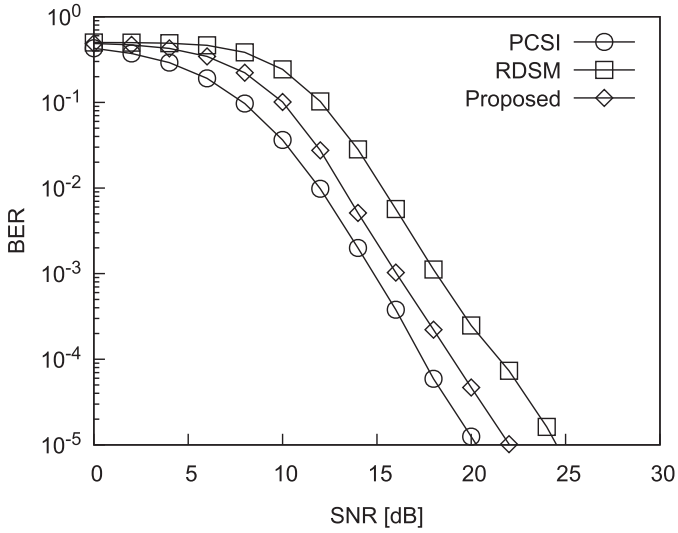

Fig. 5. The BER performance of the proposed scheme with $(M, N) = (256, 4)$. The frame length was given by $T = 5120$, and the transmission rate was $R = 10$ [bps/Hz]. The normalized Doppler frequency was $F_d T_s = 10^{-5}$.

VI. Conclusion

We proposed the variable-block-length joint CE and DD for SM, where the block length is set to shorter than the channel's coherence time. The MSE bounds of CE, as well as the detection complexity, was characterized for the proposed scheme. Our simulation results demonstrated that the proposed SM scheme approached that with PCSI, especially in slow fading channels, while outperforming the recent RDSM scheme without any significant penalty in terms of preamble overhead and detection complexity. Furthermore, the benefit of the proposed scheme over the RDSM scheme increased upon increasing the Doppler frequency.

References

[1] T. L. Marzetta, "Noncooperative cellular wireless with unlimited numbers of base station antennas," *IEEE Trans. Wireless Commun.*, vol. 9, no. 11, pp. 3590–3600, Nov. 2010.
[2] J. G. Andrews *et al.*, "What will 5G be?," *IEEE J. Sel. Areas Commun.*, vol. 32, no. 6, pp. 1065–1082, Jun. 2014.
[3] S. Sugiura, S. Chen, and L. Hanzo, "A universal space-time architecture for multiple-antenna aided systems," *IEEE Commun. Surveys Tut.*, vol. 14, no. 2, pp. 401–420, May 2012.
[4] M. Di Renzo, H. Haas, A. Ghrayeb, S. Sugiura, and L. Hanzo, "Spatial modulation for generalized MIMO: Challenges, opportunities and implementation," *Proc. IEEE*, vol. 102, no. 1, pp. 1–47, Jan. 2014.
[5] S. Sugiura, T. Ishihara, and M. Nakao, "State-of-the-art design of index modulation in the space, time, and frequency domains: Benefits and fundamental limitations," *IEEE Access*, vol. 5, pp. 21 774–21 790, 2017.
[6] M. Wen *et al.*, "A survey on spatial modulation in emerging wireless systems: Research progresses and applications," *IEEE J. Sel. Areas Commun.*, vol. 37, no. 9, pp. 1949–1972, Sep. 2019.
[7] M. Arisaka and S. Sugiura, "Energy-versus-bandwidth-efficiency trade-off in spatially modulated massive MIMO downlink," *IEEE Wireless Commun. Lett.*, vol. 8, no. 1, pp. 197–200, Feb. 2018.
[8] M. Di Renzo, D. D. Leonardis, F. Graziosi, and H. Haas, "Space shift keying (SSK) MIMO with practical channel estimates," *IEEE Trans. Commun.*, vol. 60, no. 4, pp. 998–1012, Apr. 2012.
[9] S. Sugiura and L. Hanzo, "Effects of channel estimation on spatial modulation," *IEEE Signal Process. Lett.*, vol. 19, no. 12, pp. 805–808, Dec. 2012.
[10] X. Wu, H. Claussen, M. Di Renzo, and H. Haas, "Channel estimation for spatial modulation," *IEEE Trans. Commun.*, vol. 62, no. 12, pp. 4362–4372, Dec. 2014.

[11] Y. M. Khattabi and S. A. Alkhawaldeh, "Performance analysis of spatial modulation under rapidly time-varying Rayleigh fading channels," *IEEE Access*, vol. 7, pp. 110 594–110 604, 2019.
[12] C. Cozzo and B. L. Hughes, "Joint channel estimation and data detection in space-time communications," *IEEE Trans. Commun.*, vol. 51, no. 8, pp. 1266–1270, Aug. 2003.
[13] S. Buzzi, M. Lops, and S. Sardellitti, "Performance of iterative data detection and channel estimation for single-antenna and multiple-antennas wireless communications," *IEEE Trans. Veh. Technol.*, vol. 53, no. 4, pp. 1085–1104, Jul. 2004.
[14] M. Abuthinien, S. Chen, and L. Hanzo, "Semi-blind joint maximum likelihood channel estimation and data detection for MIMO systems," *IEEE Signal Process. Lett.*, vol. 15, pp. 202–205, Jan. 2008.
[15] S. Chen, S. Sugiura, and L. Hanzo, "Semi-blind joint channel estimation and data detection for space-time shift keying systems," *IEEE Signal Process. Lett.*, vol. 17, no. 12, pp. 993–996, Dec. 2010.
[16] L. Hanzo, Y. Akhtman, L. Wang, and M. Jiang, *MIMO-OFDM for LTE, WIFI and WIMAX: Coherent Versus Non-Coherent and Cooperative Turbo-Tranceivers*, Chichester, West Sussex, U.K.: John Wiley and IEEE Press, 2011.
[17] N. Ishikawa and S. Sugiura, "Unified differential spatial modulation," *IEEE Wireless Commun. Letters*, vol. 3, no. 4, pp. 337–340, Aug. 2014.
[18] N. Ishikawa and S. Sugiura "Rectangular differential spatial modulation for open-loop noncoherent massive-MIMO downlink," *IEEE Trans. Wireless Commun.*, vol. 16, no. 3, pp. 1908–1920, Mar. 2017.
[19] R. Penrose, "A generalized inverse for matrices," in *Mathematical Proc. of the Cambridge Philos. Society*, vol. 51, no. 3, 1955, pp. 406–413.
[20] T. V. H. Nguyen, S. Sugiura, and K. Lee, "Low-complexity sphere search-based adaptive spatial modulation," *IEEE Trans. Veh. Technol.*, vol. 67, no. 8, pp. 7836–7840, Aug. 2018.
[21] N. Ishikawa, S. Sugiura, and L. Hanzo, "Subcarrier-index modulation aided OFDM - will it work?," *IEEE Access*, vol. 4, pp. 2580–2593, 2016.
[22] M. Wen, Q. Li, E. Basar, and W. Zhang, "Generalized multiple-mode OFDM with index modulation," *IEEE Trans. Wireless Commun.*, vol. 17, no. 10, pp. 6531–6543, Oct. 2018.